Fully Ionized Quasi-One-Dimensional Magnetic Nozzle Flow

DONALD L. CHUBB*
NASA Lewis Research Center, Cleveland, Ohio

Theme

TO investigate magnetic nozzle processes, a quasi-one-dimensional analysis was employed that included the effects of unequal electron and ion temperatures and electron-thermal conductivity.

Content

Plasma devices such as the external field MPD arc and the Q-machine wind tunnel produce high-speed flows in a diverging magnetic field. One possible explanation for the acceleration mechanism in these devices is that the applied diverging magnetic field acts as a nozzle. Axial acceleration occurs as a result of both the magnetic pressure exerted by the nozzle and the conversion of thermal motion into axially directed motion.

The geometry of the problem considered in this study is shown in Fig. 1. An imposed axially-symmetric magnetic field controls the flow. Any change in the magnetic field from induced currents is neglected.

One fairly simple method of analyzing this plasma flow is by a quasi-one-dimensional analysis similar to those applied in ordinary gasdynamics. In the case of a fully-ionized plasma, however, we must consider two species (ions and electrons) rather than a single species. Also, the electrons tend to have a higher temperature than the ions. The small electron mass results in large values of the thermal conductivity for the electrons. Therefore, in the analysis herein, unequal electron and ion temperatures, as well as electron-thermal conductivity, are included. The quasi-one-dimensional equations were derived by integrating the various equations over the control volume shown in Fig. 1 (this is a segment of the nozzle). Also, the following assumptions are made: 1) Plasma properties are uniform across the nozzle, 2) No current in x direction, $J_x = 0$, 3) Quasi-neutrality, $n_e = n_i$, 4) Heat flux in r and θ directions is negligible, 5) Viscous forces are negligible, 6) No energy added to flow, and 7) Ratio of electron to ion mass, $m_e/m_i = \varepsilon^2$, negligible compared to 1. It should be noted that 1 is the basic assumption for any quasi-one-dimensional analysis.

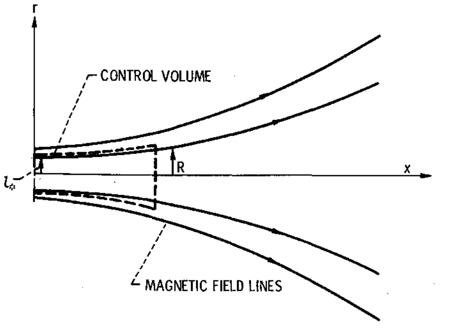

Fig. 1 Magnetic nozzle.

Presented as Paper 71-141 at the AIAA 9th Aerospace Sciences Meeting, New York, January 25–27, 1971; submitted February 10, 1971; synoptic received April 21, 1971; revision received September 9, 1971. Full paper is available from AIAA. Price: AIAA members, $1.50; nonmembers, $2.00. Microfiche, $1.00. **Orders must be accompanied by remittance.**

Index categories: Plasma Dynamics and MHD; Electric and Advanced Space Propulsion; Nozzle and Channel Flow.

* Research Engineer. Member AIAA.

Under the above assumptions, the following dimensionless equations are obtained.

$$\left(\frac{5}{3}M_*{}^2-\frac{T_0}{V^2}\right)\frac{dV}{dx}+\frac{1}{V}\frac{dT_0}{dx}=G(x)+\frac{T_0}{AV}\frac{dA}{dx} \quad \text{Plasma Momentum} \tag{1}$$

$$\tfrac{5}{3}M_*{}^2V(dV/dx)+\tfrac{5}{2}(dT_0/dx)+(\tfrac{6}{5})^{1/2}(A/\varepsilon M_*)(dq/dx)=0 \quad \text{Plasma Energy} \tag{2}$$

$$\frac{T_e}{V}\frac{dV}{dx}+\frac{3}{2}\frac{dT_e}{dx}+\left(\frac{6}{5}\right)^{1/2}\frac{A}{\varepsilon M_*}\frac{dq}{dx}=3\left(\frac{l_*}{\lambda_{ei_*}}\right)\frac{\varepsilon}{M_*}\frac{v}{V}(T_0-2T_e)-\frac{T_e}{A}\frac{dA}{dx} \quad \text{Electron Energy} \tag{3}$$

$$(\tfrac{6}{5})^{1/2}(5T_e/4AV)(dT_e/dx)=-1.866(l_*/\lambda_{ei_*})vq \quad \text{Heat Flux} \tag{4}$$

The plasma continuity equation was used to eliminate ρ and $p = nk(T_e+T_i)$ was used to eliminate p in Eqs. (1–4). The dimensionless quantities appearing in Eqs. (1–4) are $x = \bar{x}/l_*$ axial coordinate, $V = \bar{V}/\bar{V}_*$ axial velocity, $T_e = \bar{T}_e/\bar{T}_*$ electron temperature. $T_0 = (\bar{T}_e+\bar{T}_i)/\bar{T}_*$ total temperature, $v = \bar{v}/\bar{v}_{ei_*} = 1/AVT_e^{3/2}$ collision frequency, $A = \bar{A}/\pi\bar{l}_*{}^2$ nozzle area, $q = 2\bar{q}_x/m_e\bar{n}_*(2k\bar{T}_*/m_e)^{3/2}$ axial-electron heat flux. $M_*{}^2 = 3m_i\bar{V}_*{}^2/5kT_*$ throat Mach number, $\lambda_{ei_*} = (5k\bar{T}_*/3m_e)^{1/2}/v_{ei_*}$ collisional mean-free path at throat, $\varepsilon^2 = m_e/m_i$ ratio of electron to ion masses, and $\beta_* = 2\bar{n}_*k\bar{T}_*/\mu_0\bar{B}_{x_*}{}^2$ ratio of kinetic pressure to magnetic pressure at throat. The asterisk is used to denote conditions that exist at the nozzle throat. Barred quantities are dimensional, $\bar{T}_* = (\bar{T}_0)_{x=0}$ and l_* is the throat radius.

The magnetic field is assumed to determine the nozzle shape, therefore,

$$d\bar{R}/d\bar{x} = \bar{B}_r/\bar{B}_x \tag{5}$$

where $\bar{R}$ is the nozzle radius at position x. Also, from $\nabla\cdot\mathbf{B} = 0$ and assuming B_x is uniform across the nozzle

$$\bar{B}_x\bar{A} = (\bar{B}_x\bar{A})_{x=0} \tag{6}$$

from Eqs. (5), (6), and $\bar{A} = \pi\bar{R}^2$;

$$G(x) \equiv -\frac{A}{\beta_*}\frac{dB_r{}^2}{dx} = \frac{1}{4\beta_*A^2}\frac{dA}{dx}\left[\frac{3}{A}\left(\frac{dA}{dx}\right)^2-2\frac{d^2A}{dx^2}\right] \tag{7}$$

In the definition of $G(x)$, the magnetic pressure $dB_r{}^2/dx$ is an average over the cross-sectional area.

The nozzle radius dependence on x was assumed to be the following

$$\bar{R} = a\bar{x}^p + l_* \tag{8}$$

As a result,

$$(1/A)(dA/dx) = 2pA_s[x^{p-1}/(A_sx^p+1)] \tag{9}$$

$$G = [2p^2(p-1)/\beta_*]A_s{}^2[A_sx^p(p+1)/(p-1)-1]x^{2p-3}/(A_sx^p+1)^3 \tag{10}$$

where

$$A_s = al_*{}^{p-1} \tag{11}$$

The set of Eqs. (1–4) has a singularity at the point where flow Mach number satisfies the following expression

$$M^2 = m_i\bar{V}^2/\tfrac{5}{3}k\bar{T}_0 = M_e{}^2/(M_e{}^2+\tfrac{2}{5}\varepsilon^2) \tag{12}$$

where

$$M_e^{\,2} = m_e \bar{V}^2/\tfrac{5}{3}k\bar{T}_e \tag{13}$$

Equation (12) shows that the singular point occurs at a subsonic Mach number. One way of making the flow pass smoothly through this singular point is to fix it at the throat ($dA/dx = 0$) and also require the heat flux at the throat to satisfy the following expression

$$q_* = (25/18.66)(\tfrac{6}{5})^{1/2}(\varepsilon T_{e_*}/M_*)(2T_{e_*} - 1) \tag{14}$$

If the singularity is at the throat Eq. (12) yields,

$$M_*^{\,2} = 1 - \tfrac{2}{5}T_{e_*} \tag{15}$$

since $V_* = 1$. It should be pointed out that the conditions $dA/dx = 0$ and q satisfying Eq. (14) are imposed conditions that allow a smooth transition through the singular point. An actual flow in the given nozzle may establish the singular point at a different location.

Since T_{e_*} is a boundary condition on the electron temperature it might at first seem that solutions should be obtainable for all values of T_{e_*} from 0 to 1. However, it was found that for given values of the other parameters a physically meaningful solution was obtained for only one value of T_{e_*}. By a physically meaningful solution, one means a solution in which $T_e \leq T_0$ for large values of x.

It is of interest to compare the solution of Eqs. (1–4) with the adiabatic and isentropic flows for a similar nozzle. To obtain the adiabatic solution, we merely let $q = 0$. In this case, the maximum velocity ratio that can be obtained for a monatomic gas is $(V_{\max})_{ad} = 2$.

For isentropic flow, $q = 0$, and no current may flow in the plasma. The magnetic field term G results frm the $\mathbf{J} \times \mathbf{B}$ term in the plasma momentum equation. Therefore, since $J \rightarrow 0$, $G \rightarrow 0$ as well. Under these conditions, the usual one-dimensional isentropic flow equations for a monatomic gas ($\gamma = \frac{5}{3}$) are obtained.

The equations were integrated using the Runge-Kutta method. The integration was started near the throat of the nozzle ($x = 0$). Since the throat is at the critical point, it is not possible to begin the integration at exactly $x = 0$. However, it was found that different starting points very close to $x = 0$ did not greatly effect the solution obtained. For all the cases presented here, the following starting values were used; $x = 0.001$, $V = 1.0001$, and $T_0 = 1.0$. An iterative process was necessary to establish the proper value of the initial electron temperature T_{e_*}. The critical heat flux q_*, and Mach number M_*, were calculated using Eqs. (14) and (15), respectively. Solutions were obtained for various values of the parameters β_* and (l_*/λ_{ei_*}) in argon ($\varepsilon = 3.71 \times 10^{-3}$).

In Fig. 2, the complete solution is compared to the adiabatic and isentropic solutions for $A_s = 0.02$, $p = 2$, $\beta_* = 5$, and $(l_*/\lambda_{ei_*}) = 5$. The velocity and temperature profiles for the adiabatic and isentropic cases are nearly the same. That is why they are shown together in Fig. 2. There are two significant things to notice from these results. First of all, velocities higher than the adiabatic limit can be attained when $q \neq 0$. Secondly, the electron temperature, and likewise the total temperature, remains relatively high throughout the nozzle. The cause of this temperature result is the large thermal conductivity for the electrons.

Changing β_*, while keeping the other parameters constant, results in only a slight change in the velocity and heat-flux profiles. Increasing β_* produces a small increase in the velocity. The temperature profiles show a greater change with β_*. Larger values of β_* result in higher temperatures throughout the nozzle. Such a result is expected since large values of β_* mean that the thermal energy density is large compared to the magnetic energy density.

The effect of the collision parameter l_*/λ_{ei_*}, is more pronounced than β_*. Increasing the value of l_*/λ_{ei*} produces lower values for V, T_0, T_e, and q. Large values of l_*/λ_{ei_*} imply a more collisional flow. As the flow becomes more collisional, the electron-thermal conductivity is decreased. Therefore, the flow approaches the adiabatic limit and the resulting lower values for V, T_0, T_e, and q.

Plasma properties have been measured in the magnetic nozzle of a low-power MPD arc. It is difficult to compare these experimental results with the theory since the values of β_* and l_*/λ_{ei_*} appropriate to the experiment are not known. However, there is qualitative agreement between the theory and experiment for the electron temperature. The experimental electron temperature decreases much slower than that in an adiabatic expansion which is in agreement with the theory.

The significant results of this analysis are the prediction of higher velocities and temperatures than a corresponding adiabatic flow. Both of these results occur because of the inclusion of the electron-thermal conductivity.

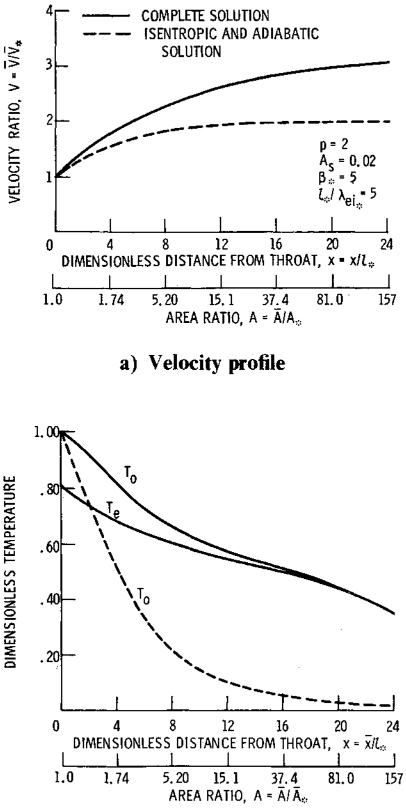

b) Temperature profiles

Fig. 2 Comparison of solution with adiabatic and isentropic solutions. Magnetic nozzle parameters, $p = 2$ and $A_s = 0.02$, ratio kinetic to magnetic pressure $\beta_* = 5$, collision parameter $l_*/\lambda_{ei_*} = 5$.